Hindawi Publishing Corporation
International Journal of Antennas and Propagation
Volume 2014, Article ID 506457, 13 pages
http://dx.doi.org/10.1155/2014/506457

Research Article

Application of a Channel Estimation Algorithm to Spectrum Sensing in a Cognitive Radio Context

Vincent Savaux,[1] Moïse Djoko-Kouam,[2] Yves Louët,[1] and Alexandre Skrzypczak[3]

[1] *IETR-Supélec, 35000 Rennes, France*
[2] *ECAM Rennes-Louis de Broglie, 35170 Rennes, France*
[3] *Zodiac Data Systems, 14000 Caen, France*

Correspondence should be addressed to Vincent Savaux; vincent.savaux@supelec.fr

Received 7 November 2013; Accepted 27 January 2014; Published 26 March 2014

Academic Editor: Ali El-Hajj

This paper deals with spectrum sensing in an orthogonal frequency division multiplexing (OFDM) context, allowing an opportunistic user to detect a vacant spectrum resource in a licensed band. The proposed method is based on an iterative algorithm used for the joint estimation of noise variance and frequency selective channel. It can be seen as a second-order detector, since it is performed by means of the minimum mean square error criterion. The main advantage of the proposed algorithm is its capability to perform spectrum sensing, noise variance estimation, and channel estimation in the presence of a signal. Furthermore, the sensing duration is limited to only one OFDM symbol. We theoretically show the convergence of the algorithm, and we derive its analytical detection and false alarm probabilities. Furthermore, we show that the detector is very efficient, even for low SNR values, and is robust against a channel uncertainty.

1. Introduction

Wireless communications are facing a constant increase of data-rate-consuming transmissions, due to the multiplications of the applications and services, while the available spectrum resource is naturally limited. Furthermore, most of the frequency bands are already allocated to specific licenses. However, some of these licensed bands are not used at their full capacity, which results in spectrum holes along the time and frequency axes [1], whereas they could be exploited in order to achieve the requirements of data rate. Away from the usual paradigm in which the channels are allocated only for licensed users, Mitola and Maguire Jr. defined the cognitive radio [2], allowing an opportunistic access by unlicensed users to the unused frequency bands. In such network, the opportunistic users, called secondary users (SUs), can use licensed bands when primary users (PUs) are not active. The main condition for the SUs to use the licensed bands is to minimize the interferences with PUs. Thus, they must be able to sense the presence of the PUs, even if the PU's signal is attenuated compared to the noise level. Figure 1 depicts the concept of spectrum sensing: a PU transmitter (PU-Tx) is transmitting to a PU receiver (PU-Rx) while a SU transmitter intends to transmit in the same band. In order to avoid the interferences with the PU, the SU has to perform spectrum sensing. In order to lighten the drawing, only one PU-Rx and two SU-Rxs are depicted, but the network can obviously be more complex. The process set up by the SUs to sense the presence of the PUs is called spectrum sensing. The authors of [3–5] propose detailed reviews of the different techniques of spectrum sensing. The different methods are usually classified into two main categories: the cooperative detection and the noncooperative detection. In this paper, we take an interest in the latter.

The noncooperative detection concerns a sole SU who tries to detect the presence of the PU alone. Among the wide range of methods [3–6], one can describe the main ones: the energy detector measures the energy of the received signal and compares it to a threshold. It has a low complexity of implementation and does not require any knowledge on the PU's signal features. However, the choice of the threshold value depends on the noise variance, and the uncertainties

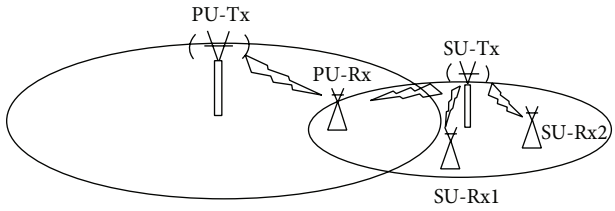

Figure 1: Illustration of the principle of the spectrum sensing.

on the noise level may cause important degradations of the detector performance [7, 8]. The matched-filter correlates the received signal with the one transmitted by the PU, which is supposed to be known at the receiver [9, 10]. This is the optimal detector when the signal is transmitted with AWGN only and supposed to be known at the receiver. Due to these hypotheses, this method is generally not applicable in practice, and its performance is degraded when the knowledge of the signal is erroneous [11]. Less binding than the matched-filter, the feature detectors only use several characteristics of the signal to detect the PU. Thus, the waveform-based sensing uses the preamble of the PU's signal (used for the synchronization, the estimation, etc.) to perform a correlation with the received signal [12]. However, the performance of the waveform-based sensing is degraded in the presence of selective channels. In the same way, when a CP is used in an OFDM signal, its autocorrelation function becomes time-varying, so a second-order-based method consists of detecting the peaks in the autocorrelation function at time-lag T_s. More generally, the cyclostationarity detector exploits the periodic redundancy of all telecommunications signals to differentiate it from a pure Gaussian noise [13, 14]. As indicated in [5], the redundancy can occur due to periodic patterns such as the CP, the symbol rate, or the channel code. However, these second-order detectors require large sensing time, that is, a large number of symbols to be performed. In [15], a hybrid architecture composed of both energy and cyclostationarity is proposed. It allows the energy detector to compensate its limitation due to the noise uncertainty thanks to a cyclostationarity detection stage whose computation time is reduced. Another attractive technique called eigenvalue-based detection uses the characteristics of the covariance matrix of large-sized random matrices (e.g., containing noise samples only) [16–18]. Indeed, the random matrix theory proved that the distribution of the eigenvalues of such matrix tends to a deterministic function. In [16], if the noise variance is known, the signal is detected if a peak appears outside of the domain of the function. Using the same theory, the authors of [17] propose the maximum-minimum eigenvalue (MME) detection, whose principle consists of comparing the ratio between the maximum and minimum eigenvalues with a threshold to take the decision. Based on the same theory, both techniques have the same asymptotic performance, but the latter does not require the noise level to be performed. However, these two methods require matrices with very large sizes, hence, a large number of sensors and a long sensing time. In order to use MME detection with a single sensor, the authors of [19] propose to artificially create a large matrix by stacking the shifted vectors of the received sampled signal. However, this method is limited since the rows of the created matrix are correlated.

In this paper, we propose to perform spectrum sensing by means of a minimum mean square error (MMSE-)based iterative algorithm developed in [20] for the joint estimation of noise variance and frequency selective channel. Since we consider a sole receiver, the context of the next sections will be the noncooperative detection of a PU transmitting an OFDM signal by a single SU in a given narrow band. In the presence or absence of signal, the algorithm converges after a few iterations and performs the estimation of the noise variance. We then add a metric to the method presented in [20] in order to turn it into a spectrum sensing algorithm. The metric is defined by the difference between the second-order moment M_2 of the received signal and the estimated noise variance. If the PU is present (resp. absent), the metric is equal to the power of the transmitted signal (resp. equal to zero). As the algorithm is based on MMSE criterion, it requires the estimation of the channel covariance matrix, so the detector can be classified as a second-order statistics detector. Compared to usual second-order statistics detectors such as MME, the proposed one only needs the time duration of one OFDM symbol to be performed. It is also robust in frequency selective channels context. Furthermore, when the PU's signal is present, it achieves a joint estimation of noise variance and channel. When the PU is absent, it also performs the noise variance estimation, and it is proved that it reaches the exact noise power value. In this paper, a theoretical expression of the detection and the false alarm probabilities are derived, and we show that they are very close to the simulations.

In this paper, the normal font x is used for scalar variables, the boldface $\mathbf{x}$ is used for vectors, and the underlined boldface $\underline{\mathbf{x}}$ is used for matrices. Furthermore, small letters x point out the variables in the time domain and capital letters X in the frequency domain.

This paper is organized as follows: Section 2 presents the system model and the algorithm developed in [20]. In Section 3, we prove the convergence of the algorithm in the absence of the signal, and we characterize the detector in Section 4. In Section 5, we give the theoretical expressions of the false alarm and detection probabilities. Simulations results are depicted in Section 6, and finally we draw our conclusions in Section 7.

2. Background

2.1. System Model. We consider the problem of the detection of an OFDM pilot preamble over a Rayleigh fading channel with additive white Gaussian noise (AWGN) in a given band. After the M-points discrete Fourier transform (DFT), the received signal is noted $\mathbf{U}$. According to the presence or the absence of the primary user (PU) in the band, the usual hypothesis test is given by

$$\begin{aligned} \mathbb{H}_0 &: \mathbf{U} = \mathbf{W}, \\ \mathbb{H}_1 &: \mathbf{U} = \underline{\mathbf{C}}\mathbf{H} + \mathbf{W}, \end{aligned} \tag{1}$$

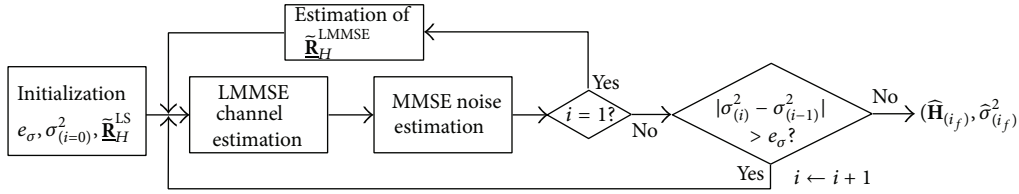

Figure 2: Block diagram of the iterative algorithm in the realistic scenario.

where $\mathbb{H}_0$ and $\mathbb{H}_1$ denote the absence and the presence of the PU hypotheses, respectively. According to the model given in [20], the variable $\mathbf{H}$ is the $M \times 1$ complex vector of the frequency response of the channel, composed of the frequency response samples H_m, $m = 0, 1, \ldots, M-1$:

$$H_m = \sum_{l=0}^{L-1} h_l \exp\left(-2j\pi \frac{m\tau_l}{M}\right), \tag{2}$$

where L is the number of paths of the channel and h_l and τ_l are the zero-mean Gaussian path coefficients and the sampled path delays, respectively. We assume that the channel $\mathbf{H}$ follows a wide sense stationary uncorrelated scattering (WSSUS) model [21]. Consequently, $|H_m|$ follows a Rayleigh distribution. The variable $\underline{\mathbf{C}}$ is the $M \times M$ diagonal matrix composed of the pilots C_m such that $|C_m| = 1$, without loss of generality, and $\mathbf{W}$ is the $M \times 1$ vector of AWGN with variance σ^2. Let us assume that, under hypothesis $\mathbb{H}_1$, the receiver is synchronized on the position of the preamble $\underline{\mathbf{C}}$.

2.2. Iterative Algorithm for the Channel and Noise Variance Estimation. We now briefly recall the steps of the algorithm for the joint and iterative estimation of the channel and the noise variance as given in [20], that is, under the hypothesis $\mathbb{H}_1$. Basically, it is an MMSE-based iterative algorithm in which, at each step, the noise variance estimation feeds the channel estimation and vice versa. In addition to the noise variance, the linear-MMSE (LMMSE) channel estimation [22] requires the channel covariance matrix that has to be estimated at the receiver. This estimated channel covariance matrix is noted $\widetilde{\underline{\mathbf{R}}}_H$. The algorithm from [20] is described by Figure 2 and its steps are detailed in the following.

(1) At the beginning, only the LS channel estimation $\widehat{\mathbf{H}}^{\text{LS}}$ performed on a pilot preamble is available at the receiver, so the only way to estimate the covariance matrix denoted by $\widetilde{\underline{\mathbf{R}}}_H^{\text{LS}}$ is

$$\widetilde{\underline{\mathbf{R}}}_H^{\text{LS}} = \widehat{\mathbf{H}}^{\text{LS}}\left(\widehat{\mathbf{H}}^{\text{LS}}\right)^H, \tag{3}$$

where $(\cdot)^H$ is the Hermitian transposition. Furthermore, a stopping criterion e_σ is fixed. Let us denote i to be the index of the iteration.

(2) At the first step ($i = 1$) of the algorithm, the LMMSE channel estimation [22, 23] is performed with $\widetilde{\underline{\mathbf{R}}}_H^{\text{LS}}$:

$$\widehat{\mathbf{H}}_{(i=1)}^{\text{LMMSE}} = \widetilde{\underline{\mathbf{R}}}_H^{\text{LS}}\left(\widetilde{\underline{\mathbf{R}}}_H^{\text{LS}} + \widehat{\sigma}^2_{(i=0)}\underline{\mathbf{C}}\underline{\mathbf{C}}^H\right)^{-1}\widehat{\mathbf{H}}^{\text{LS}}, \tag{4}$$

where $\widehat{\sigma}^2_{(i=0)}$ points out the initialization value of the noise variance and $\underline{\mathbf{C}}\underline{\mathbf{C}}^H$ is equal to the identity matrix $\underline{\mathbf{I}}$.

(3) The noise variance is estimated by means of the MMSE criterion [24] $\widehat{\sigma}^2_{(i=1)} = (1/M)E\{\|\widehat{\mathbf{H}}^{\text{LS}} - \widehat{\mathbf{H}}\|^2\}$, with $\widehat{\mathbf{H}} = \widehat{\mathbf{H}}_{(i=1)}^{\text{LMMSE}}$:

$$\widehat{\sigma}^2_{(i=1)} = \frac{1}{M}E\left\{\left\|\widehat{\mathbf{H}}^{\text{LS}} - \widehat{\mathbf{H}}_{(i=1)}^{\text{LMMSE}}\right\|^2\right\}, \tag{5}$$

with $\|\cdot\|$ being the Frobenius matrix norm, defined by $\|\underline{\mathbf{A}}\| = \sqrt{\text{tr}(\underline{\mathbf{A}}\underline{\mathbf{A}}^H)}$. If the algorithm keeps on computing with $\widetilde{\underline{\mathbf{R}}}_H^{\text{LS}}$, it is proved in [20] that $(\widehat{\sigma}^2_{(i)})$ converges to zero. Under this condition, the algorithm enters into an endless loop. This is due to the fact that $\widetilde{\underline{\mathbf{R}}}_H^{\text{LS}}$ is sensitive to the noise and then it is a rough approximation of the exact covariance matrix. In order to obtain a more accurate channel covariance matrix, it is now possible to use $\widehat{\mathbf{H}}_{(i=1)}^{\text{LMMSE}}$, such that

$$\widetilde{\underline{\mathbf{R}}}_H^{\text{LMMSE}} = \widehat{\mathbf{H}}_{(i=1)}^{\text{LMMSE}}\left(\widehat{\mathbf{H}}_{(i=1)}^{\text{LMMSE}}\right)^H. \tag{6}$$

(4) For $i \geq 2$, the iterative estimation steps (4) and (6) are performed by using (6):

$$\widehat{\mathbf{H}}_{(i)}^{\text{LMMSE}} = \widetilde{\underline{\mathbf{R}}}_H^{\text{LMMSE}}\left(\widetilde{\underline{\mathbf{R}}}_H^{\text{LMMSE}} + \widehat{\sigma}^2_{(i-1)}\underline{\mathbf{I}}\right)^{-1}\widehat{\mathbf{H}}^{\text{LS}}, \tag{7}$$

$$\widehat{\sigma}^2_{(i)} = \frac{1}{M}E\left\{\left\|\widehat{\mathbf{H}}^{\text{LS}} - \widehat{\mathbf{H}}_{(i)}^{\text{LMMSE}}\right\|^2\right\}. \tag{8}$$

It will be shown afterwards that the characterization of the initialization $\widehat{\sigma}^2_{(i=0)}$ remains the same in the presence or absence of the PU. However, it is already obvious that $\widehat{\sigma}^2_{(i=0)}$ must be strictly positive; otherwise, $\widehat{\mathbf{H}}_{(i)}^{\text{LMMSE}} = \widehat{\mathbf{H}}^{\text{LS}}$ in (7). In that case, $\widehat{\sigma}^2_{(i)} = 0$, and the algorithm enters into an endless loop.

(5) While $|\widehat{\sigma}^2_{(i)} - \widehat{\sigma}^2_{(i-1)}| > e_\sigma$, go back to Step 4 with $i \leftarrow i+1$; otherwise, go to Step 6.

(6) End of the algorithm. We note i_f to be the index of the last iteration.

It is proved in [20] that this algorithm converges if the initialization value of the noise variance is chosen such that $\widehat{\sigma}^2_{(i=0)} \gg M_2$, where M_2 is the second-order moment of the received signal $\mathbf{U}$. Moreover, the algorithm converges to limits $(\widehat{\mathbf{H}}_{(i_f)}, \widehat{\sigma}^2_{(i_f)})$ that are close to the exact values $(\mathbf{H}, \sigma^2)$. From (4) and (7) we can deduce the complexity of the algorithm. The LMMSE channel estimation requires M^3 scalar multiplications for the matrix inversion

and multiplication and the noise variance M^2. The covariance matrices estimation also requires M^2 operations. Finally, we then evaluate the complexity of the proposed algorithm by $\mathcal{O}(i_f M^3)$.

Unlike the presented model, the next section investigates the behavior of the algorithm when the PU is absent, that is, under hypothesis $\mathbb{H}_0$.

3. Convergence of the Iterative Algorithm under Hypothesis $\mathbb{H}_0$

The signal $\underline{\mathbf{C}}$ is now supposed to be absent, so the received signal is $\mathbf{U} = \mathbf{W}$. The convergence of the proposed algorithm in the case of absence of signal is going to be proved. Furthermore, it will be proved afterwards that the nonnull solution allows to turn the MMSE-based algorithm into a free band detector. To this end, the first four steps of the iterative algorithm presented in Section 2.2 are expressed under hypothesis $\mathbb{H}_0$.

3.1. Expression of the Algorithm under $\mathbb{H}_0$. Let us consider that the receiver does not know if the signal is present or absent, so the same formalism as in Section 2.2 is used, and the steps of the algorithm are recalled by considering noise only. At the beginning of the process, the LS channel estimation has been performed, $\widehat{\mathbf{H}}^{\mathrm{LS}} = \underline{\mathbf{C}}^{-1}\mathbf{U} = \underline{\mathbf{C}}^{-1}\mathbf{W}$. The following steps are as follows.

(1) From $\widehat{\mathbf{H}}^{\mathrm{LS}}$, the channel covariance matrix is estimated by

$$\widetilde{\underline{\mathbf{R}}}_H^{\mathrm{LS}} = \widehat{\mathbf{H}}^{\mathrm{LS}}\left(\widehat{\mathbf{H}}^{\mathrm{LS}}\right)^H = \mathbf{W}\mathbf{W}^H. \tag{9}$$

Additionally, a stopping criterion e_σ and an initialization $\widehat{\sigma}^2_{(i=0)}$ are set.

(2) At iteration $i = 1$ of the algorithm, the LMMSE channel estimation $\widehat{\mathbf{H}}^{\mathrm{LMMSE}}_{(i=1)}$ is performed by using $\widetilde{\underline{\mathbf{R}}}_H^{\mathrm{LS}}$:

$$\widehat{\mathbf{H}}^{\mathrm{LMMSE}}_{(i=1)} = \underline{\mathbf{R}}_H^{\mathrm{LS}}\left(\underline{\mathbf{R}}_H^{\mathrm{LS}} + \widehat{\sigma}^2_{(i=0)}\underline{\mathbf{I}}\right)^{-1}\widehat{\mathbf{H}}^{\mathrm{LS}}. \tag{10}$$

(3) The MMSE noise variance estimation $\widehat{\sigma}^2_{(i=1)}$ is performed with $\widehat{\mathbf{H}} = \widehat{\mathbf{H}}^{\mathrm{LMMSE}}_{(i=1)}$:

$$\widehat{\sigma}^2_{(i=1)} = \frac{1}{M}E\left\{\left\|\widehat{\mathbf{H}}^{\mathrm{LS}} - \widehat{\mathbf{H}}^{\mathrm{LMMSE}}_{(i=1)}\right\|^2\right\}, \tag{11}$$

and a new covariance matrix is computed by

$$\widetilde{\underline{\mathbf{R}}}_H^{\mathrm{LMMSE}} = \widehat{\mathbf{H}}^{\mathrm{LMMSE}}_{(i=1)}\left(\widehat{\mathbf{H}}^{\mathrm{LMMSE}}_{(i=1)}\right)^H. \tag{12}$$

Indeed, it is proved in the Appendix that if the algorithm keeps on computing with $\widetilde{\underline{\mathbf{R}}}_H^{\mathrm{LS}} = \mathbf{W}\mathbf{W}^H$, then the sequence $\widehat{\sigma}^2_{(i)}$ necessarily converges to zero. When $\widetilde{\underline{\mathbf{R}}}_H^{\mathrm{LS}}$ is used, and in spite of its inputs being different, the algorithm has exactly the same response whatever the hypothesis, $\mathbb{H}_0$ or $\mathbb{H}_1$.

(4) Then, for $i \geq 2$, iteratively perform the channel and the noise variance estimation:

$$\widehat{\mathbf{H}}^{\mathrm{LMMSE}}_{(i)} = \widetilde{\underline{\mathbf{R}}}_H^{\mathrm{LMMSE}}\left(\widetilde{\underline{\mathbf{R}}}_H^{\mathrm{LMMSE}} + \widehat{\sigma}^2_{(i-1)}\underline{\mathbf{I}}\right)^{-1}\widehat{\mathbf{H}}^{\mathrm{LS}}, \tag{13}$$

$$\widehat{\sigma}^2_{(i)} = \frac{1}{M}E\left\{\left\|\widehat{\mathbf{H}}^{\mathrm{LS}} - \widehat{\mathbf{H}}^{\mathrm{LMMSE}}_{(i)}\right\|^2\right\}. \tag{14}$$

From these first four steps of the algorithm, it is now possible to prove that the algorithm converges to a nonnull solution under $\mathbb{H}_0$.

3.2. Scalar Expression of the Sequence $(\widehat{\sigma}^2_{(i)})$ under $\mathbb{H}_0$. The convergence of the algorithm is now going to be proved, and its limit characterized. To this end, we will first obtain a scalar expression of the sequence $(\widehat{\sigma}^2_{(i)})$. We use the Hermitian property of $\widetilde{\underline{\mathbf{R}}}_H^{\mathrm{LS}} = \left(\widetilde{\underline{\mathbf{R}}}_H^{\mathrm{LS}}\right)^H$, and we develop (12) with (10) to get

$$\begin{aligned}
\widetilde{\underline{\mathbf{R}}}_H^{\mathrm{LMMSE}} &= \widehat{\mathbf{H}}^{\mathrm{LMMSE}}_{(i=1)}\left(\widehat{\mathbf{H}}^{\mathrm{LMMSE}}_{(i=1)}\right)^H \\
&= \widetilde{\underline{\mathbf{R}}}_H^{\mathrm{LS}}\left(\widetilde{\underline{\mathbf{R}}}_H^{\mathrm{LS}} + \widehat{\sigma}^2_{(i=0)}\underline{\mathbf{I}}\right)^{-1}\widehat{\mathbf{H}}^{\mathrm{LS}} \\
&\quad\times\left(\widetilde{\underline{\mathbf{R}}}_H^{\mathrm{LS}}\left(\widetilde{\underline{\mathbf{R}}}_H^{\mathrm{LS}} + \widehat{\sigma}^2_{(i=0)}\underline{\mathbf{I}}\right)^{-1}\widehat{\mathbf{H}}^{\mathrm{LS}}\right)^H \\
&= \widetilde{\underline{\mathbf{R}}}_H^{\mathrm{LS}}\left(\widetilde{\underline{\mathbf{R}}}_H^{\mathrm{LS}} + \widehat{\sigma}^2_{(i=0)}\underline{\mathbf{I}}\right)^{-1}\widehat{\mathbf{H}}^{\mathrm{LS}}\left(\widehat{\mathbf{H}}^{\mathrm{LS}}\right)^H \\
&\quad\times\left(\widetilde{\underline{\mathbf{R}}}_H^{\mathrm{LS}}\left(\widetilde{\underline{\mathbf{R}}}_H^{\mathrm{LS}} + \widehat{\sigma}^2_{(i=0)}\underline{\mathbf{I}}\right)^{-1}\right).
\end{aligned} \tag{15}$$

Let us assume that M is large enough to justify the approximation $\mathrm{tr}(\mathbf{W}\mathbf{W}^H) = \mathrm{tr}(\sigma^2\underline{\mathbf{I}})$. Since the estimation of the noise variance is calculated by means of the trace in (14), we make the assumption that as a first approximation $\widetilde{\underline{\mathbf{R}}}_H^{\mathrm{LS}} \approx \sigma^2\underline{\mathbf{I}}$, and then it is possible to replace $\underline{\mathbf{R}}_H^{\mathrm{LMMSE}}$ by

$$\begin{aligned}
\widetilde{\underline{\mathbf{R}}}_H^{\mathrm{LMMSE}} &= \sigma^2\underline{\mathbf{I}}\left(\sigma^2\underline{\mathbf{I}} + \widehat{\sigma}^2_{(i=0)}\underline{\mathbf{I}}\right)^{-1}\widetilde{\underline{\mathbf{R}}}_H^{\mathrm{LS}}\left(\sigma^2\underline{\mathbf{I}}\left(\sigma^2\underline{\mathbf{I}} + \widehat{\sigma}^2_{(i=0)}\underline{\mathbf{I}}\right)^{-1}\right) \\
&= \frac{\sigma^6}{\left(\sigma^2 + \widehat{\sigma}^2_{(i=0)}\right)^2}\underline{\mathbf{I}}
\end{aligned} \tag{16}$$

in (14). Thus, by reinjecting (16) in (13) and (14), it yields

$$\begin{aligned}\widehat{\sigma}^2_{(i+1)} &= \frac{1}{M}E\left\{\left\|\widehat{\mathbf{H}}^{\mathrm{LS}} - \widehat{\mathbf{H}}^{\mathrm{LMMSE}}_{(i+1)}\right\|^2\right\}\\ &= \frac{1}{M}E\left\{\left\|\widehat{\mathbf{H}}^{\mathrm{LS}} - \underline{\widetilde{\mathbf{R}}}^{\mathrm{LMMSE}}_{H}\right.\right.\\ &\qquad\left.\left.\times\left(\underline{\widetilde{\mathbf{R}}}^{\mathrm{LMMSE}}_{H} + \widehat{\sigma}^2_{(i)}\underline{\mathbf{I}}\right)^{-1}\widehat{\mathbf{H}}^{\mathrm{LS}}\right\|^2\right\}\\ &= \frac{1}{M}E\left\{\left\|\mathbf{W} - \frac{\sigma^6}{\left(\sigma^2+\widehat{\sigma}^2_{(i=0)}\right)^2}\underline{\mathbf{I}}\right.\right.\\ &\qquad\left.\left.\times\left(\frac{\sigma^6}{\left(\sigma^2+\widehat{\sigma}^2_{(i=0)}\right)^2}\underline{\mathbf{I}} + \widehat{\sigma}^2_{(i)}\underline{\mathbf{I}}\right)^{-1}\mathbf{W}\right\|^2\right\} \quad (17)\\ &= \frac{1}{M}E\left\{\left\|\left(\widehat{\sigma}^2_{(i)}\underline{\mathbf{I}}\left(\left(\frac{\sigma^6}{\left(\sigma^2+\widehat{\sigma}^2_{(i=0)}\right)^2}\right.\right.\right.\right.\\ &\qquad\left.\left.\left.\left.+\widehat{\sigma}^2_{(i)}\right)\underline{\mathbf{I}}\right)^{-1}\right)\mathbf{W}\right\|^2\right\}\\ &= \frac{\sigma^2\widehat{\sigma}^4_{(i)}\left(\sigma^2+\widehat{\sigma}^2_{(i=0)}\right)^4}{\left(\sigma^6+\widehat{\sigma}^2_{(i)}\left(\sigma^2+\widehat{\sigma}^2_{(i=0)}\right)^2\right)^2}.\end{aligned}$$

For a better readability, we note the following mathematical developments:

$$A = \sigma^2 + \widehat{\sigma}^2_{(i=0)}. \quad (18)$$

3.3. Convergence of the Sequence $(\widehat{\sigma}^2_{(i)})$ to a Nonnull Solution. One can observe that the sequence $(\widehat{\sigma}^2_{(i+1)})$ is built from a function f_{s1} such that if we note $x = \widehat{\sigma}^2_{(i)}$, we have

$$f_{s1}(x) = \frac{\sigma^2A^4x^2}{\left(\sigma^6 + A^2x\right)^2}. \quad (19)$$

The sequence converges if f_{s1} has at least one fixed point. Zero is an obvious fixed point, but it has been proved in the Appendix that the algorithm enters into an endless loop if $(\widehat{\sigma}^2_{(i)})$ converges to zero. We then solve the equation $f_{s1}(x) = x$ to find the other fixed points:

$$\begin{aligned}&f_{s1}(x) = x\\ &\Longleftrightarrow \frac{\sigma^2A^4x^2}{\left(\sigma^6 + A^2x\right)^2} = x\\ &\Longleftrightarrow \sigma^2A^4x^2 = x\left(\sigma^6 + A^2x\right)^2.\end{aligned} \quad (20)$$

Since we exclude zero as a solution, the previous expressions can be simplified by x, and the problem amounts to look for real roots of the polynomial $A^4x^2 + x(2A^2\sigma^6 - \sigma^2A^4) + \sigma^{12}$. Since it is a second order polynomial, in order to find real solutions, the first condition on the initialization $\widehat{\sigma}^2_{(i=0)}$ is to obtain the discriminant $\Delta = (2A^2\sigma^6 - \sigma^2A^4)^2 - 4A^4\sigma^{12}$ positive; that is,

$$\begin{aligned}\Delta \geq 0 &\Longleftrightarrow \left(2A^2\sigma^6 - \sigma^2A^4\right)^2 \geq 4A^4\sigma^{12}\\ &\Longleftrightarrow A^2 \geq 4\sigma^4\\ &\Longleftrightarrow \left(\sigma^2 + \widehat{\sigma}^2_{(i=0)}\right)^2 \geq 4\sigma^4\\ &\Longleftrightarrow \widehat{\sigma}^2_{(i=0)} \geq 3\sigma^2.\end{aligned} \quad (21)$$

As σ^2 is absolutely unknown, one can find a stronger condition on $\widehat{\sigma}^2_{(i=0)}$, conditionally to $\Delta > 0$. We then find the roots r^+_s and r_{s-} of the polynomial under the condition $\Delta > 0$:

$$\begin{aligned}r^+_{s-} &= \frac{\left(\sigma^2A^4 - 2A^2\sigma^6\right) \pm \sqrt{\left(2A^2\sigma^6 - \sigma^2A^4\right)^2 - 4A^4\sigma^{12}}}{2A^4}\\ &\Longleftrightarrow r^+_{s-} = \frac{\left(\sigma^2A^2 - 2\sigma^6\right) \pm \sqrt{\sigma^4A^4 - 4\sigma^8A^2}}{2A^2}.\end{aligned} \quad (22)$$

If we notice that when $\widehat{\sigma}^2_{(i=0)}$ tends to $+\infty$, then $A = \sigma^2 + \widehat{\sigma}^2_{(i=0)}$ also tends to $+\infty$, we get

$$\begin{aligned}\lim_{A\to\infty} r^+_s &= \frac{\sigma^2A^2 + \sigma^2A^2}{2A^2} = \sigma^2,\\ \lim_{A\to\infty} r_{s-} &= \frac{\sigma^2A^2 - \sigma^2A^2}{2A^2} = 0.\end{aligned} \quad (23)$$

It can be seen that by choosing a sufficiently large initialization value $\widehat{\sigma}^2_{(i=0)}$, the sequence $(\widehat{\sigma}^2_{(i)})$ converges to a value as close as possible to the exact value of the noise variance σ^2. This characterization of the initialization value $\widehat{\sigma}^2_{(i=0)}$ perfectly tallies with the one made for the sufficient condition in [20]; that is, $\widehat{\sigma}^2_{(i=0)} \gg M_2$. Moreover, it will be further shown that this condition allows to differentiate $\mathbb{H}_0$ from $\mathbb{H}_1$. Thus, choosing $\widehat{\sigma}^2_{(i=0)}$ with a large value is the condition for the algorithm to converge to a nonnull solution for both hypotheses $\mathbb{H}_0$ and $\mathbb{H}_1$. Besides that, since it converges, the stopping criterion $|\widehat{\sigma}^2_{(i)} - \widehat{\sigma}^2_{(i-1)}| < e_\sigma$ can also be the same under $\mathbb{H}_0$. Finally, the MMSE-based algorithm can be used as a free band detector.

Figure 3 displays the function f_{s1} for different values of $(\widehat{\sigma}^2_{(i=0)})$, compared with $y = x$ and for a fixed value $\sigma^2 = 1$. By comparing the curves of f_{s1} for different initializations values, we verify that the larger the value of $\widehat{\sigma}^2_{(i=0)}$, the closer $\widehat{\sigma}^2_{(i_f)}$ to the real value of σ^2.

4. Proposed Detector

4.1. Decision Rule for the Proposed Detector. In this section, a decision rule for the detector is proposed. To this end, whatever $\mathbb{H}_0$ or $\mathbb{H}_1$, it is supposed that the algorithm has

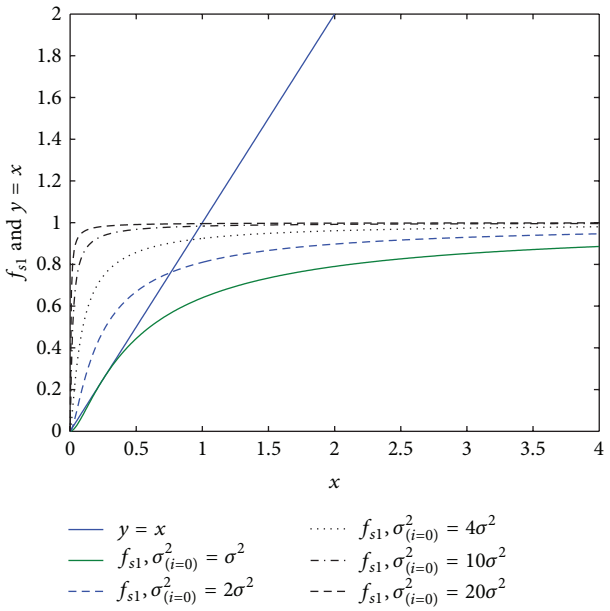

FIGURE 3: Aspect of f_{s1} for different values of $\sigma^2_{(0)}$, $\sigma^2 = 1$ compared with $y = x$.

converged; that is, the condition $|\widehat{\sigma}^2_{(i)} - \widehat{\sigma}^2_{(i-1)}| < e_\sigma$ is reached and then $i = i_f$. The second-order moment $M_2 = (1/M)\sum_{m=0}^{M-1} |U_m|^2$ of the received signal is expressed under the hypotheses $\mathbb{H}_0$ and $\mathbb{H}_1$:

$$M_2 = \begin{cases} \dfrac{1}{M}\displaystyle\sum_{m=0}^{M-1} |W_m|^2, & \text{if } \mathbb{H}_0 \\ \dfrac{1}{M}\displaystyle\sum_{m=0}^{M-1} |C_m H_m + W_m|^2, & \text{if } \mathbb{H}_1. \end{cases} \tag{24}$$

The second-order moment M_2 is the decision metric used for the energy detector. Here, a different metric noted $\mathscr{M}$ is proposed and defined by

$$\mathscr{M} = \left| M_2 - \widehat{\sigma}^2 \right|, \tag{25}$$

where $\widehat{\sigma}^2 = \widehat{\sigma}^2_{(i_f)}$ is the noise variance estimation performed by the proposed iterative algorithm. From (24), the metric (25) is rewritten according to the hypotheses $\mathbb{H}_0$ and $\mathbb{H}_1$:

$$\mathscr{M} = \begin{cases} \left| \dfrac{1}{M}\displaystyle\sum_{m=0}^{M-1} |W_m|^2 - \widehat{\sigma}^2 \right|, & \text{under } \mathbb{H}_0 \\ \left| \dfrac{1}{M}\displaystyle\sum_{m=0}^{M-1} |C_m H_m + W_m|^2 - \widehat{\sigma}^2 \right|, & \text{under } \mathbb{H}_1. \end{cases} \tag{26}$$

By fixing a threshold ς, the decision criterion is now

$$\begin{aligned} &\mathbb{H}_0, \quad \text{if } \mathscr{M} < \varsigma, \\ &\mathbb{H}_1, \quad \text{else.} \end{aligned} \tag{27}$$

The detection and false alarm probabilities are defined by

$$\begin{aligned} P_d &= P\left(\mathscr{M} > \varsigma \mid \mathbb{H}_1\right), \\ P_{\text{fa}} &= P\left(\mathscr{M} > \varsigma \mid \mathbb{H}_0\right). \end{aligned} \tag{28}$$

The detection probability P_d is the probability to decide $\mathbb{H}_1$ while the PU is present, and the false alarm probability P_{fa} is the probability to decide $\mathbb{H}_1$ while the PU is absent. As mentioned in [6, 25], the sensibility of the detector (the expected value of P_{fa} and P_d) depends on the application. In a cognitive radio context, the SU has to minimize the interference with the PU, so the probability of detection has to be maximized, whereas if the false alarm probability is not optimized, it only implies that the SU misses white spaces. On the contrary, in a radar application, a false alarm could have serious consequences, especially in a military context.

4.2. Expression of the Proposed Detector. By taking into account the previous decision rule, it is possible to extend the practical algorithm proposed in the scenario of the joint estimation of the SNR and the channel for free band detections, as it is summed up in Algorithm 1.

It can be seen that the structure of Algorithm 1 is similar to the one of [20] and summarized in Section 2.2, but with a detection part. Thus, compared to the methods of the literature, the proposed one not only returns the decision $\mathbb{H}_0$ and $\mathbb{H}_1$ but also provides

(i) the noise variance estimation, if $\mathbb{H}_0$;

(ii) the channel and SNR estimations, if $\mathbb{H}_1$.

An a priori qualitative analysis of the detector can be done. Indeed, from (26), one can deduce that by supposing a good estimation of $\widehat{\sigma}^2$, $\mathscr{M}$ tends to a value close to zero under $\mathbb{H}_0$ and to a value close to P_s under $\mathbb{H}_1$. By supposing a normalized signal power, one can suppose that choosing a value ς between zero and one allows getting a viable detector. Concerning the value of the threshold e_σ, since it ensures the convergence of the algorithm, it has no effect on the detector performance. This property will be shown by simulations afterward.

In the context of cognitive radio, the SUs have to target a given detection probability, noted P_d^t. Thus, according to the Neyman-Pearson criterion [26], the best value of the threshold ς can be analytically derived (when it is possible) by solving $P(\mathscr{M} > \varsigma \mid \mathbb{H}_1) \geq P_d^t$ and by maximizing the likelihood ratio test (LRT)

$$\Lambda(x) = \frac{p\left(x \mid \mathbb{H}_1\right)}{p\left(x \mid \mathbb{H}_0\right)} \underset{\mathbb{H}_0}{\overset{\mathbb{H}_1}{\gtrless}} \varsigma. \tag{29}$$

To this end, the probability density functions (pdfs) of $\mathscr{M}$ have to be expressed, which is proposed in the next section.

begin
Initialization: $\widetilde{\underline{\mathbf{R}}}_H^{\mathrm{LS}}$, $e_\sigma > 0$, $\widehat{\sigma}^2_{(i=0)}$ and ς;
$i \leftarrow 1$;
while $\left|\widehat{\sigma}^2_{(i)} - \widehat{\sigma}^2_{(i-1)}\right| > e_\sigma$ **do**
if $i = 1$ **then**
Perform LMMSE channel estimation;
Perform the noise variance estimation;
Calculate the matrix $\widetilde{\underline{\mathbf{R}}}_H^{\mathrm{LMMSE}}$;
else
Perform an LMMSE channel estimation with $\widetilde{\underline{\mathbf{R}}}_H^{\mathrm{LMMSE}}$;
Perform the noise variance estimation;
end
$i \leftarrow i + 1$;
end
Calculate the metric $\mathscr{M}$;
if $\mathscr{M} < \varsigma$ **then**
return $\mathbb{H}_0$;
else
return $\mathbb{H}_1$;
end
end

Algorithm 1: Application of the MMSE-based algorithm to free band detection.

5. Detection and False Alarm Probabilities

5.1. Probability Density Function of $\mathscr{M}$ under $\mathbb{H}_1$. Under the hypothesis $\mathbb{H}_1$, since it is proved in [20] that the noise variance estimation is very accurate, it is reasonable to suppose that the noise variance estimation is good enough to consider that $\widehat{\sigma}^2 \approx (1/M)\sum_{m=0}^{M-1}|W_m|^2$, so the contribution of $C_m H_m$ is prevailing in $\mathscr{M}$ (26) so that

$$\begin{aligned}\mathscr{M} &= \left|\frac{1}{M}\sum_{m=0}^{M-1}\left(\left|C_m H_m + W_m\right|^2\right) - \widehat{\sigma}^2\right| \\ &= \left|\frac{1}{M}\sum_{m=0}^{M-1}\left(\left|C_m H_m\right|^2 + \left|W_m\right|^2 + \mathrm{CF}_m\right) - \widehat{\sigma}^2\right|,\end{aligned} \tag{30}$$

where $\forall m = 0, \ldots, M-1$, CF_m are the cross-factors $(C_m H_m W_m^*) + (C_m H_m W_m^*)^*$, whose means (for a sufficiently large value of M) are equal to zero, since H_m and W_m are zero-mean uncorrelated Gaussian processes. The development of (30) then simply yields

$$\begin{aligned}\mathscr{M} &= \left|\frac{1}{M}\sum_{m=0}^{M-1}\left|C_m H_m\right|^2 + \left|W_m\right|^2 - \widehat{\sigma}^2\right| \\ &= \frac{1}{M}\sum_{m=0}^{M-1}\left|H_m C_m\right|^2.\end{aligned} \tag{31}$$

The result in (31) obtained with the approximation $\widehat{\sigma}^2 \approx (1/M)\sum_{m=0}^{M-1}|W_m|^2$ may be debated, since it has been proved in [20] that the noise estimation under hypothesis $\mathbb{H}_1$ is slightly biased. However, it will be shown in Section 6 that this approximation is accurate for low values of σ^2. From the channel frequency response expression (2) and remembering that $C_m C_m^* = 1$, the metric (31) can be rewritten by

$$\begin{aligned}\mathscr{M} &= \frac{1}{M}\sum_{m=0}^{M-1}\left|\sum_{l=0}^{L-1} h_l \exp\left(-2j\pi\frac{m\beta_l}{M}\right) C_m\right|^2 \\ &= \frac{1}{M}\sum_{m=0}^{M-1}\left(\sum_{l_1=0}^{L-1} h_{l_1}\exp\left(-2j\pi\frac{m\beta_{l_1}}{M}\right) C_m\right) \\ &\qquad \times \left(\sum_{l_2=0}^{L-1} h_{l_2}\exp\left(-2j\pi\frac{m\beta_{l_2}}{M}\right) C_m\right)^* \\ &= \sum_{l=0}^{L-1}\left|h_l\right|^2 \\ &\quad + \frac{1}{M}\sum_{m=0}^{M-1}\sum_{l_1=0}^{L-1}\sum_{\substack{l_2=0 \\ l_2\neq l_1}}^{L-1} h_{l_1} h_{l_2}^* \exp\left(-2j\pi\frac{m\left(\beta_{l_1} - \beta_{l_2}\right)}{M}\right).\end{aligned} \tag{32}$$

According to the Rayleigh distributed WSSUS channel model, whatever $l = 0, \ldots, L-1$, the gains h_l are uncorrelated zero-mean Gaussian processes. For a large enough value M, let us assume that the mean of the cross-factors of the right side in (32) are equal to zero. Finally, the metric $\mathscr{M}$ is simply written as follows:

$$\mathscr{M} = \sum_{l=0}^{L-1}\left|h_l\right|^2, \quad \text{under } \mathbb{H}_1. \tag{33}$$

$\mathscr{M}$ then follows a chi-square distribution with $2L$ degrees of freedom. The probability density function (pdf) noted $p_{\mathscr{M}}(x)$ of the decision statistic under $\mathbb{H}_1$ is then expressed by

$$p_{\mathscr{M}}(x) = \frac{1}{2^L P_s^L \Gamma(L)} x^{L-1} \exp\left(-\frac{x}{2P_s}\right), \quad \text{under } \mathbb{H}_1, \quad (34)$$

where $\Gamma(\cdot)$ is the gamma function [27].

5.2. Probability Density Function of $\mathscr{M}$ under $\mathbb{H}_0$. The theoretical probability density function (pdf) expression of the metric under the hypothesis $\mathbb{H}_0$

$$\mathscr{M} = \left| \frac{1}{M} \sum_{m=0}^{M-1} |W_m|^2 - \widehat{\sigma}_{(i)}^2 \right| \quad (35)$$

is now developed. To this end, let us assume that the initialization value of the algorithm is chosen large enough to state $\widehat{\sigma}^2 \approx \sigma^2$, in accordance with the previously formulated hypotheses in Section 3.3. Whatever $m = 0, \ldots, M-1$, each sample W_m follows a zero-mean Gaussian process with variance σ^2; $|W_m|^2$ has a chi-square distribution χ_2^2 with a degree of liberty equal to 2:

$$\chi_2^2(x) = \frac{1}{\sigma^2} e^{-x/\sigma^2}. \quad (36)$$

The mean and the variance of this distribution are equal to σ^2 and σ^4, respectively. In an OFDM context, we reasonably suppose that M is large enough (e.g., $M > 100$) to consider that from the central limit theorem $(1/M)\sum_{m=0}^{M-1} |W_m|^2$ follows a normal distribution $\mathcal{N} \sim (\sigma^2, \sigma^4/M)$, and then $(1/M)\sum_{m=0}^{M-1} |W_m|^2 - \widehat{\sigma}^2$ follows a centered normal distribution $\mathcal{N} \sim (0, \sigma^4/M)$. Consequently, the metric $\mathscr{M} = |(1/M)\sum_{m=0}^{M-1} |W_m|^2 - \widehat{\sigma}_{(i)}^2|$ has a chi distribution χ_1 with one degree of liberty:

$$p_{\mathscr{M}}(x) = \frac{\sqrt{2}}{\Gamma(1/2)\sqrt{\sigma^4/M}} \exp\left(-\frac{1}{2}\left(\frac{x}{\sqrt{\sigma^4/M}}\right)^2\right), \quad \text{under } \mathbb{H}_0. \quad (37)$$

As a conclusion, the probability density functions of the metric $\mathscr{M}$, according to $\mathbb{H}_0$ and $\mathbb{H}_1$, are given by

$$p_{\mathscr{M}}(x) = \begin{cases} \dfrac{\sqrt{2}}{\Gamma(1/2)\sqrt{\sigma^4/M}} \exp\left(-\dfrac{1}{2}\left(\dfrac{x}{\sqrt{\sigma^4/M}}\right)^2\right), & \text{under } \mathbb{H}_0 \\ \dfrac{1}{2^L P_s^L \Gamma(L)} x^{L-1} \exp\left(-\dfrac{x}{2P_s}\right), & \text{under } \mathbb{H}_1. \end{cases} \quad (38)$$

5.3. Analytical Expressions of P_d and P_{fa}. The detection and false alarm probabilities P_d and P_{fa} are obtained by integrating (38) between the fixed threshold ς and $+\infty$. For the calculation of P_d, the solution is derived in [28, 29]:

$$\begin{aligned} P_d &= P(\mathscr{M} > \varsigma \mid \mathbb{H}_1) \\ &= \int_{\varsigma}^{+\infty} \frac{x^{L-1}}{2^L P_s^L \Gamma(L)} \exp\left(-\frac{x}{2P_s}\right) dx \\ &= \frac{\Gamma(L, \varsigma/2P_s)}{\Gamma(L)}, \end{aligned} \quad (39)$$

where $\Gamma(\cdot,\cdot)$ is the incomplete gamma function [27]. In the case $\mathbb{H}_0$, we have

$$\begin{aligned} P_{\text{fa}} &= \int_{\varsigma}^{+\infty} p_{\mathscr{M}}(x)\, dx \\ &= \int_{\varsigma}^{+\infty} \frac{\sqrt{2}}{\Gamma(1/2)\sqrt{\sigma^4/M}} e^{-(1/2)(x/\sqrt{\sigma^4/M})^2} dx. \end{aligned} \quad (40)$$

By using the variable change $X = x/\sqrt{2\sigma^4/M}$ and knowing that $\Gamma(1/2) = \sqrt{\pi}$, one can recognize the complementary error function $erfc(x) = 1 - erf(x)$:

$$P_{\text{fa}} = \int_{\varsigma/\sqrt{2\sigma^4/M}}^{+\infty} \frac{2}{\sqrt{\pi}} e^{-X^2} dX = erfc\left(\frac{\varsigma\sqrt{M}}{\sqrt{2}\sigma^2}\right). \quad (41)$$

Since the incomplete gamma function is not directly invertible in (39), it is not possible to derive an analytical expression of the threshold ς in function of the targeted detection probability P_d^t. However, an approximation by means of a computer calculation or a series expansion of the invert of (39) or a simple characterization of ς by simulations can be done. We will consider this third solution thereafter. Furthermore, the next section aims to characterize the performance of the proposed detection algorithm and the validity of the proposed analytical developments.

Table 1: Table of parameters of the channel model.

	Channel model			
	Path 1	Path 2	Path 3	Path 4
Delay	0 ms	0.7 ms	1.5 ms	2.2 ms
Gain	0.7448	0.5214	0.3724	0.1862

6. Simulations Results

6.1. Simulations Parameters. The signal parameters used for the simulations are based on those of the digital radio mondiale (DRM/DRM+) standard [30]. This standard designs the digital radio broadcasting over the current AM/FM bands. When it is transmitted, the signal is composed of 148 independent carriers. The symbol and the cyclic prefix durations are 14.66 ms and 5.33 ms, respectively. Although the DRM standard recommends a pilot distribution in staggered rows, we consider a block-type pilot arrangement, according to the model used in [20]. The channel used in the presence of a PU is based on the *US Consortium* model of the DRM/DRM+ standard, whose path gains are normalized. The channel parameters are summed up in Table 1.

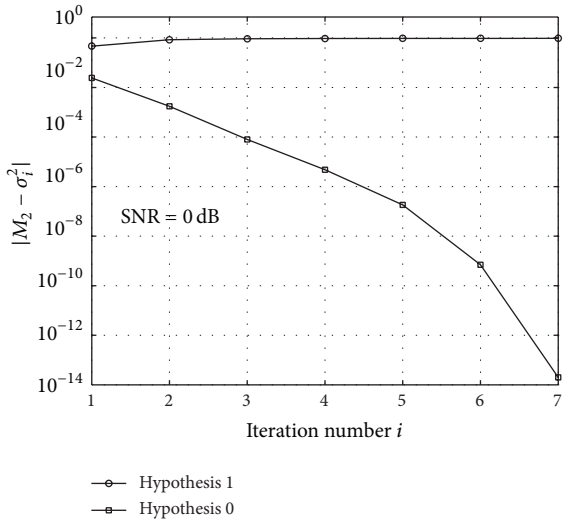

FIGURE 4: $|M_2 - \widehat{\sigma}^2|$ versus the iteration number under $\mathbb{H}_0$ and $\mathbb{H}_1$, for SNR = 0 dB.

6.2. Choice of the Threshold ς. Figure 4 depicts the metric $\mathscr{M} = |M_2 - \widehat{\sigma}^2|$ versus the number of iterations, under the hypotheses $\mathbb{H}_0$ and $\mathbb{H}_1$. The SNR is fixed equal to 0 dB. In presence of signal, the average signal power P_s is equal to 1. The simulation is performed by means of 4000 simulation runs.

It can be seen that the a priori qualitative analysis is verified. Indeed, for a sufficient number of iterations (according to the value e_σ, as shown thereafter), $\mathscr{M}$ converges to P_s under $\mathbb{H}_1$ and converges toward zero under $\mathbb{H}_0$. It has been noticed that it is not possible to find an exact value of ς according to $P(\mathscr{M} > \varsigma \mid \mathbb{H}_1) = P_d^t$. However, it is observable on Figure 4 that the choice of the threshold is not restrictive. Indeed, choosing ς as small as expected ensures a probability P_d close to one, and, for a sufficient number of iterations, it also ensures a low value for P_{fa}. Nevertheless, reducing the value of e_σ increases the number of required iterations, as shown in the following. Hence, for an expected detection probability, a tradeoff between the complexity and the acceptable level of false alarm probability has to be taken into account, since each iteration requires $\mathcal{O}(i_f M^3)$ operations.

6.3. Effect of the Choice of e_σ *on the Detector Performance.* It is shown in this section that the choice of the threshold e_σ value does not have any effect on the detection performance of the proposed method but only impacts the convergence speed of the algorithm. Figure 5 depicts the curves of detection and false alarm probabilities P_d and P_{fa} versus the SNR from −15 dB to 10 dB. In order to ensure the convergence of the algorithm, e_σ must have a low value. The subfigures (a) and (b) then depict the curves P_d and P_{fa} for $e_\sigma = 0.01$ and $e_\sigma = 0.0001$, respectively. According to the previous recommendations, the initialization $\sigma^2_{(i=0)}$ is equal to $40 \times M_2$. We also arbitrarily fix the threshold $\varsigma = 0.01$, its effect on the detection performance being further studied. The figure is obtained thanks to 2000 simulation runs.

We observe that the curves of P_d and P_{fa} match from Figures 5(a) to 5(b). P_{fa} is equal to zero or nearly for all SNR values and P_d reaches one from SNR = −5 dB. The detector can then reach the perfect one from SNR ≥ −5 dB, that is, in low SNR environment. We conclude that, assuming a value of e_σ low enough to ensure the convergence of the algorithm, this threshold does not have any effect on the detection performance of the proposed method.

Figure 6 displays the iterations number the algorithm needs before it stops versus the SNR from −10 to 10 dB. We consider three different values for the threshold: $e_\sigma = 0.01$, 0.001, and 0.0001. The simulations conditions remain the same.

Although Figures 5(a) and 5(b) display almost the same probabilities whatever the threshold e_σ, they differ from each other according to the number of iterations the algorithm requires before stopping. Indeed, remembering that we compare $|\widehat{\sigma}^2_{(i)} - \widehat{\sigma}^2_{(i-1)}|$ with e_σ, the lower e_σ, the larger the number i of iterations needed to reach e_σ. However, Figure 6 shows that the maximum mean of iterations is less than 7 for SNR = −10 dB and shows the maximum mean of iterations is less than 5 for SNR = −10 dB and $e_\sigma = 0.0001$, which is a reasonable number of iterations. We conclude that the choice of e_σ has no effect on the detector efficiency, while it allows the convergence of the algorithm. Besides this result, the number of required iterations reasonably increases when e_σ and the SNR have low values. The detector then remains usable in practice under these conditions.

6.4. Detector Performance with Channel Uncertainty. In this part, we study the behavior of the proposed detector when a non-WSS channel is considered. To this end, we artificially correlate the different paths by inserting the gain h_0 into the other path gains. Thus, from the originally created channel impulse response $[h_0, \ldots, h_{L-1}]$ with independent paths, we build a new correlated vector $[h_0, \ldots, \widetilde{h}_l, \ldots, \widetilde{h}_{L-1}]$ such that, for $l = 1, \ldots, L-1$, we define a correlation coefficient ρ_h by

$$\rho_h = \frac{E\left\{h_0 \widetilde{h}_l^*\right\}}{\sigma_0 \widetilde{\sigma}_l}, \tag{42}$$

where $\widetilde{h}_l = h_l + \alpha_l h_0$, α_l being a coefficient that is calculated in function of the expected ρ_h, and σ_0^2 and $\widetilde{\sigma}_l^2$ are the variances of h_0 and $\widetilde{h}_l$, respectively. Figure 7 displays the detection probability P_d versus the SNR for the proposed detection under a channel correlation condition. Three curves are considered: the reference ($\rho_h = 0$) and two correlated channels with $\rho_h = 0.1$ and $\rho_h = 0.5$. We observe a limited gap of 1 dB between the reference curve and the two others. We conclude that the proposed detector is robust against the channel uncertainty.

6.5. Receiver Operating Characteristic of the Detector. The performance of a detector is usually evaluated by means of the receiver operating characteristic (ROC) curves, depicting the detection probability P_d in function of the false alarm probability P_{fa}. The optimal detector is logically reached at the point ($P_{\text{fa}} = 0, P_d = 1$). The curve $P_{\text{fa}} = P_d$ is called line

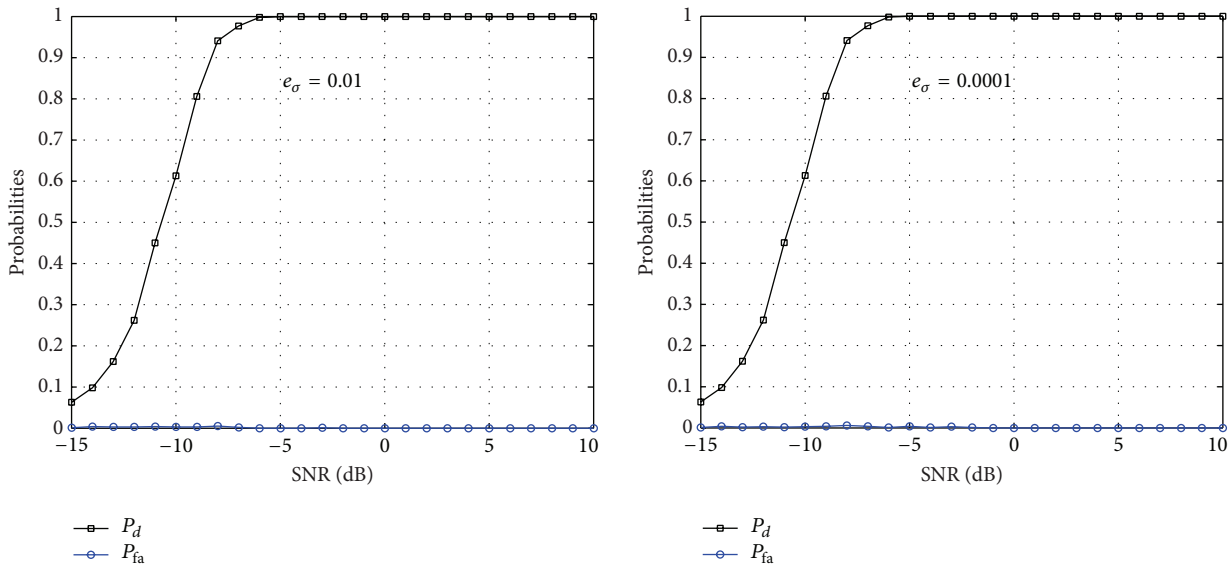

(a) P_d and P_{fa} versus SNR, for $e_\sigma = 0.01$

(b) P_d and P_{fa} versus SNR, for $e_\sigma = 0.0001$

FIGURE 5: Detection and false alarm probabilities versus SNR, for two values e_σ and for a fixed value $\varsigma = 0.01$.

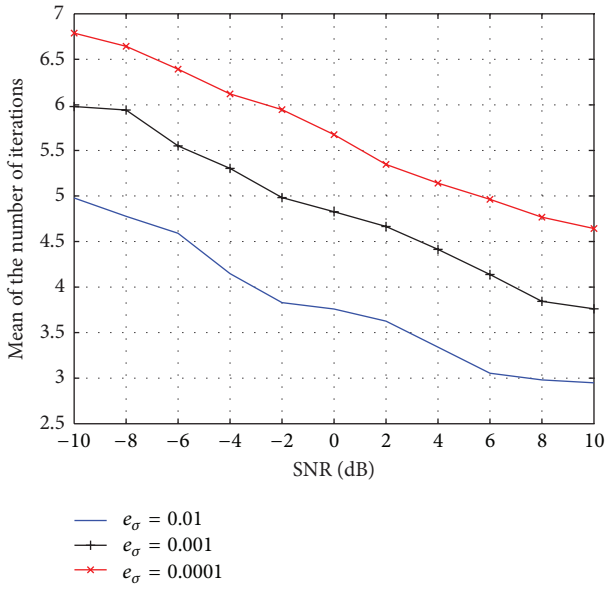

FIGURE 6: Means of the number of iterations needed by the algorithm to stop versus SNR (in dB), for three values of threshold e_σ.

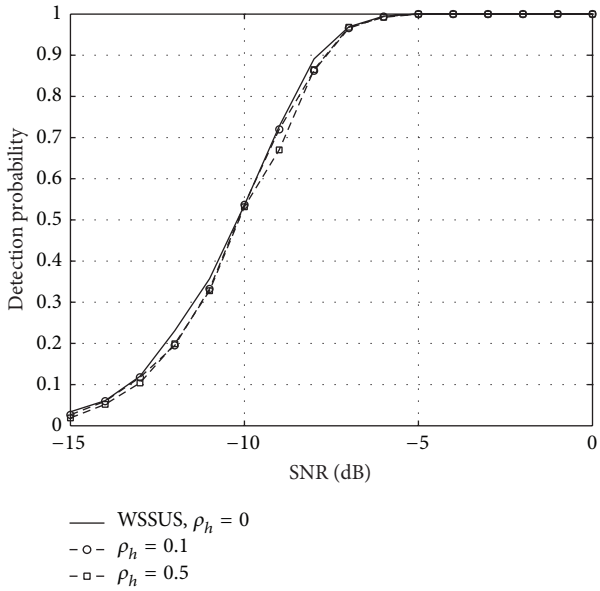

FIGURE 7: Detection probability versus SNR for a non-WSSUS channel.

of chance and corresponds to a detector that makes as much good decisions as false alarms. If the ROC curve is above the first bisector, the detector is efficient, since $P_d > P_{\text{fa}}$.

Figure 8 shows the ROC curves of the proposed detector for low SNR values (−10 dB and SNR = 0 dB). It is compared to the energy detector and the second-order moment-based MME [31]. The simulations conditions remain the same, and we fix the threshold $e_\sigma = 0.01$. In Figure 8(a), the proposed detector is compared to the usual energy detector, whose metric $\mathscr{M}$ is equal to the second order-moment of the received signal M_2. This metric is compared to a threshold ς_e to obtain the following decision rule:

$$\begin{aligned} &\mathbb{H}_0, \quad \text{if } \mathscr{M} < \varsigma_e \\ &\mathbb{H}_1, \quad \text{else.} \end{aligned} \tag{43}$$

In Figure 8(b), the proposed detector is also compared to the usual MME detector, whose metric $\mathscr{M}$ is equal to the ratio of the maximum and the nonzero minimum eigenvalues of the received signal covariance matrix $\underline{\breve{\mathbf{R}}}$; that is, $\mathscr{M} = \lambda_{\max}/\lambda_{\min}$. The same aforementioned decision rule

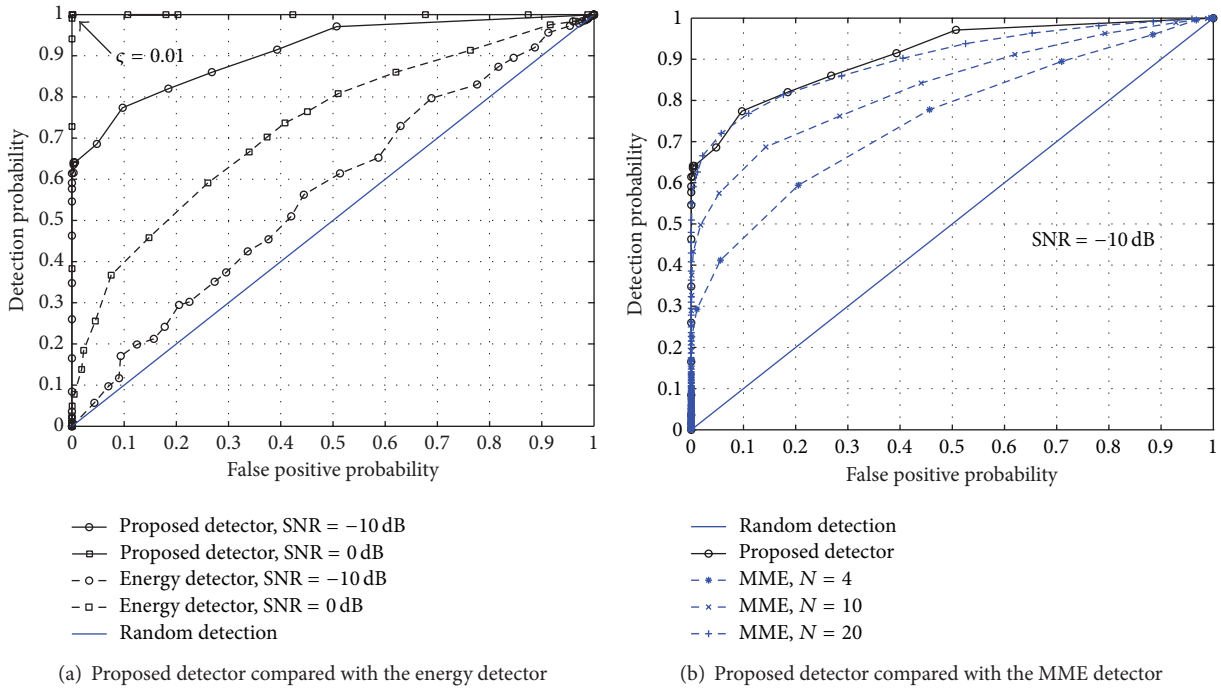

(a) Proposed detector compared with the energy detector

(b) Proposed detector compared with the MME detector

Figure 8: Receiver operating characteristic (ROC) curves of the proposed method compared to the energy and MME detectors.

is used. Since a SISO system is assumed, $\underline{\breve{\mathbf{R}}}$ is obtained by concatenating N consecutive OFDM symbols so that $\underline{\mathbf{U}}_N = [\mathbf{U}_1, \ldots, \mathbf{U}_N]$ and then $\underline{\breve{\mathbf{R}}} = \underline{\mathbf{U}}_N \underline{\mathbf{U}}_N^T$. In that way, $\underline{\mathbf{U}}_N$ is equivalent to a system with N sensors. However, due to the nature of the channel, the different received OFDM symbols are correlated. In Figure 8(b), the ROC curves of MME are obtained for $N = 4, 10$, and 20 symbols, and the SNR is equal to −10 dB. Each point of the curves is obtained by means of 2000 simulation runs.

We observe in Figure 8(a) that the proposed detector outperforms the energy detector, whatever the SNR. Indeed, as we consider the detection of a preamble transmitted over a Rayleigh channel, the power of the received signal P_S in (30) is not constant and follows a chi-square distribution. Consequently, for simulations made at a fixed SNR, the noise variance is also a varying process, which deteriorates the detector performance. For additional details about the theoretical development of the energy detection of signals with random amplitude, please refer to [28, 29]. We also may explain the performance of our detector by the fact that we use the same sensing time to compare the energy detector and the proposed algorithm, that is, only one OFDM symbol length. The 148 samples of one OFDM symbol are not enough to obtain an accurate energy detector. Figure 8(a) also confirms that the proposed detector is very efficient, since it is able to reach the perfect detector for $\varsigma = 0.01$. Indeed, for SNR = 0 dB, we observe that the ROC curve reaches the point $(P_{\text{fa}} = 0, P_d = 1)$, as we remarked in Figures 5(a) and 5(b) for SNR ≥ -5 dB. In Figure 8(b), we observe that MME requires $N = 20$ symbols to reach the performance of the proposed method, because MME is efficient for a very large size of $\underline{\mathbf{U}}_N$, and the vectors of the latter matrix are correlated. Thus, for a given performance, the complexity of MME is $\mathcal{O}(NM^2)$ (for the computation and the diagonalization of $\underline{\breve{\mathbf{R}}}$) and the one of the proposed algorithm is $\mathcal{O}(i_f M^3)$. Since we reasonably have $N < i_f M$, we conclude that the iterative method is more complex than usual second-order moment-based techniques. However, the proposed algorithm also performs the noise variance estimation if $\mathbb{H}_0$ and the SNR and channel estimation if $\mathbb{H}_1$, which is an advantage by comparison with the techniques of the literature.

Figure 9 compares the ROC curves of the proposed detector given by simulation with the theoretical ones P_d and P_{fa} given by (39) and (41), respectively. We notice that the theoretical curve for SNR = 0 dB is very close to the one obtained by simulation, whereas for SNR = −10 dB, the difference is more noticeable. This observation tallies with the discussion on the approximation $\widehat{\sigma}^2 \approx (1/M) \sum_{m=0}^{M-1} |W_m|^2$ in the calculation of the metric $\mathscr{M}$ under the hypothesis $\mathbb{H}_1$. Indeed, this approximation is justified for high values of SNR but becomes wrong for the very low SNR values. However, the theoretical curves give an idea of the detector performance for a given SNR, even for low SNR values.

7. Conclusion

In this paper, an iterative algorithm for spectrum sensing in a cognitive radio context has been presented. Originally proposed in [20] for the joint estimation of the noise and the channel, this method is based on the second-order moment of the received signal. In the presence of a primary user (PU), the algorithm estimates the channel and the noise variance. If the PU is not active, the algorithm returns a very accurate estimation of the noise level. By comparing

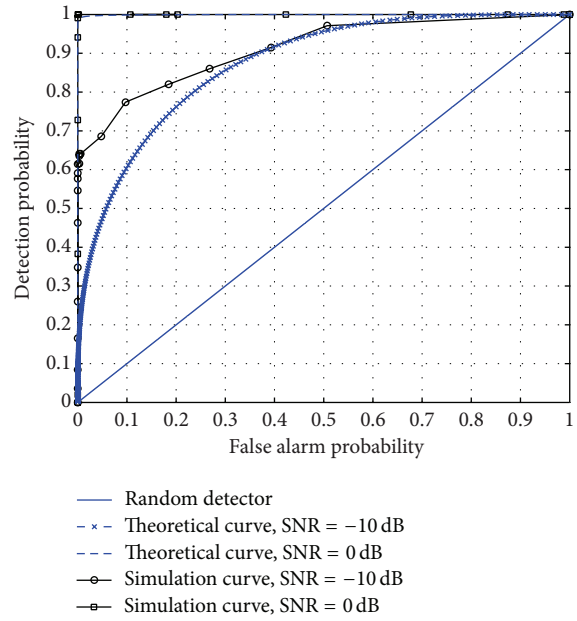

Figure 9: Comparison of the receiver operating characteristic (ROC) curves obtained by simulation and in theory.

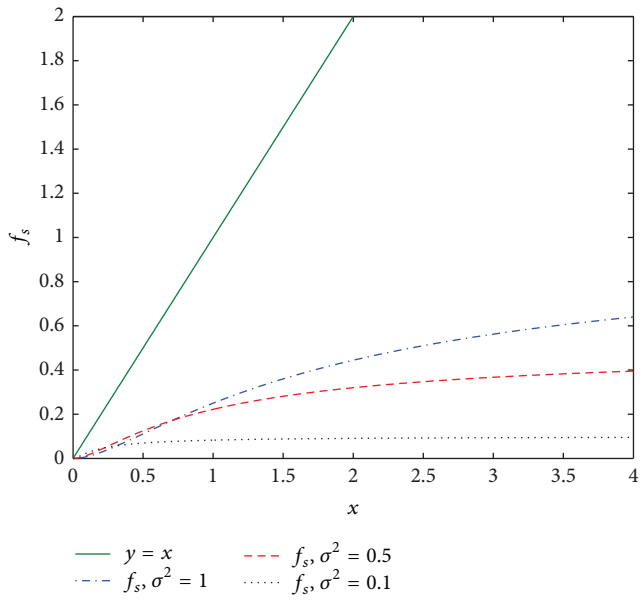

Figure 10: Aspect of f for different values of σ^2 compared with $y = x$.

the noise variance to the second moment of the received signal estimation (useful signal with noise or only noise), it is then possible to determine if the PU is present or absent. From that an analytical expression of the detection and false alarm probabilities have been proposed, and it is shown that they are very close to the simulations. It is also shown that the detector reaches the perfect one from very low SNR values. The algorithm offers numerous advantages as it performs a PU detection, the noise variance, and the channel estimation if the PU is active and it returns the noise level in the frequency band when the PU is absent, without changing the structure proposed in [20]. The future work concerning the detector will focus on the synchronization of the SU on the PU's signal.

Appendix

If the algorithm keeps on computing at each iteration i with the covariance matrix $\underline{\widetilde{\mathbf{R}}}_H^{\mathrm{LS}}$ under hypothesis $\mathbb{H}_0$, then we deduce the following for Step 4.

Perform the LMMSE channel estimation

$$\widehat{\mathbf{H}}_{(i+1)}^{\mathrm{LMMSE}} = \underline{\widetilde{\mathbf{R}}}_H^{\mathrm{LS}} \left(\underline{\widetilde{\mathbf{R}}}_H^{\mathrm{LS}} + \widehat{\sigma}_{(i)}^2 \underline{\mathbf{I}} \right)^{-1} \widehat{\mathbf{H}}^{\mathrm{LS}}. \tag{A.1}$$

Perform the MMSE noise variance estimation

$$\widehat{\sigma}_{(i+1)}^2 = \frac{1}{M} E \left\{ \left\| \widehat{\mathbf{H}}^{\mathrm{LS}} - \widehat{\mathbf{H}}_{(i+1)}^{\mathrm{LMMSE}} \right\|_F^2 \right\}. \tag{A.2}$$

It is assumed that M is large enough to get $\mathrm{tr}(\mathbf{W}\mathbf{W}^H) = \mathrm{tr}(\sigma^2 \underline{\mathbf{I}})$. We make in first approximation $\underline{\widetilde{\mathbf{R}}}_H^{\mathrm{LS}} \approx \sigma^2 \underline{\mathbf{I}}$, so the development of (A.2) yields

$$\begin{aligned} \widehat{\sigma}_{(i+1)}^2 &= \frac{1}{M} E \left\{ \left\| \widehat{\mathbf{H}}^{\mathrm{LS}} - \widehat{\mathbf{H}}_{(i+1)}^{\mathrm{LMMSE}} \right\|_F^2 \right\} \\ &= \frac{1}{M} E \left\{ \left\| \widehat{\mathbf{H}}^{\mathrm{LS}} - \underline{\widetilde{\mathbf{R}}}_H^{\mathrm{LS}} \left(\underline{\widetilde{\mathbf{R}}}_H^{\mathrm{LS}} + \widehat{\sigma}_{(i)}^2 \underline{\mathbf{I}} \right)^{-1} \widehat{\mathbf{H}}^{\mathrm{LS}} \right\|_F^2 \right\}, \end{aligned} \tag{A.3}$$

and by factorizing by $\underline{\mathbf{C}}^{-1}$:

$$\begin{aligned} &= \frac{1}{M} E \left\{ \left\| \mathbf{W} - \sigma^2 \underline{\mathbf{I}} \left(\sigma^2 \underline{\mathbf{I}} + \widehat{\sigma}_{(i)}^2 \underline{\mathbf{I}} \right)^{-1} \mathbf{W} \right\|_F^2 \right\} \\ &= \frac{1}{M} E \left\{ \left\| \left(\underline{\mathbf{I}} - \left(\sigma^2 + \widehat{\sigma}_{(i)}^2 - \widehat{\sigma}_{(i)}^2 \right) \underline{\mathbf{I}} \left(\left(\sigma^2 + \widehat{\sigma}_{(i)}^2 \right) \underline{\mathbf{I}} \right)^{-1} \right) \mathbf{W} \right\|_F^2 \right\} \\ &= \frac{1}{M} E \left\{ \left\| \left(\widehat{\sigma}_{(i)}^2 \underline{\mathbf{I}} \left(\left(\sigma^2 + \widehat{\sigma}_{(i)}^2 \right) \underline{\mathbf{I}} \right)^{-1} \right) \mathbf{W} \right\|_F^2 \right\} \\ &= \frac{\widehat{\sigma}_{(i)}^4}{\left(\sigma^2 + \widehat{\sigma}_{(i)}^2 \right)^2} \frac{1}{M} E \left\{ \| \mathbf{W} \|_F^2 \right\} \\ &= \frac{\widehat{\sigma}_{(i)}^4 \sigma^2}{\left(\sigma^2 + \widehat{\sigma}_{(i)}^2 \right)^2}. \end{aligned} \tag{A.4}$$

The sequence $(\widehat{\sigma}_{(i)}^2)$ is built from a function f_s such that if we note $x = \widehat{\sigma}_{(i)}^2$, we obtain

$$f_s(x) = \frac{x^2 \sigma^2}{\left(\sigma^2 + x \right)^2}, \tag{A.5}$$

with $x \in \mathbb{R}^+$. Figure 10 displays the curve of f_s for different values of σ^2 and compares them with $y = x$.

It is trivial that from the expression of f_s in (A.5) that the only solution of $f_s(x) = x$ is zero. We find the same results as in the case of a received pilot preamble under hypothesis

$\mathbb{H}_1$; that is, if the algorithm is exclusively performed with $\widetilde{\underline{\mathbf{R}}}_H^{\mathrm{LS}}$, then the sole limit of $\widehat{\sigma}^2_{(i+1)}$ is zero and the algorithm enters into an endless loop. It justifies the change of channel covariance matrix from $\widetilde{\underline{\mathbf{R}}}_H^{\mathrm{LS}}$ to $\widetilde{\underline{\mathbf{R}}}_H^{\mathrm{LMMSE}}$ under hypothesis $\mathbb{H}_1$ as well as under hypothesis $\mathbb{H}_0$.

Conflict of Interests

The authors declare that there is no conflict of interests regarding the publication of this paper.

References

[1] Spectrum Efficiency Working Group, "Report of the spectrum efficiency working group," Tech. Rep., Federal Communications Commission, 2002.

[2] J. Mitola III and G. Q. Maguire Jr., "Cognitive radio: making software radios more personal," *IEEE Personal Communications*, vol. 6, no. 4, pp. 13–18, 1999.

[3] T. Yücek and H. Arslan, "A survey of spectrum sensing algorithms for cognitive radio applications," *IEEE Communications Surveys and Tutorials*, vol. 11, no. 1, pp. 116–130, 2009.

[4] L. Lu, X. Zhou, U. Onunkwo, and G. Y. Li, "Ten years of research in spectrum sensing and sharing in cognitive radio," *EURASIP Journal on Wireless Communications and Networking*, vol. 2012, article 28, 2012.

[5] E. Axell, G. Leus, E. G. Larsson, and H. V. Poor, "Spectrum sensing for cognitive radio: state-of-the-art and recent advances," *IEEE Signal Processing Magazine*, vol. 29, no. 3, pp. 101–116, 2012.

[6] Z. Khalaf, *Contributions à l'étude de détection des bandes libres dans le contexte de la radio intelligente [Ph.D. thesis]*, Supélec, Rennes, France, 2013.

[7] R. Tandra and A. Sahai, "SNR walls for signal detection," *IEEE Journal on Selected Topics in Signal Processing*, vol. 2, no. 1, pp. 4–17, 2008.

[8] W. Jouini, "Energy detection limits under log-normal approximated noise uncertainty," *IEEE Signal Processing Letters*, vol. 18, no. 7, pp. 423–426, 2011.

[9] J. Proakis and M. Salehi, *Digital Communications*, McGraw-Hill, 2008.

[10] R. Price and N. Abramson, "Detection theory," *IEEE Transactions on Information Theory*, vol. 7, no. 3, pp. 135–139, 1961.

[11] A. Sahai, N. Hoven, and R. Tandra, "Some fundamental limits on cognitive radio," Proceedings of the Forty-Second Allerton Conference on Communication, Control and Computing, 2004.

[12] H. Tang, "Some physical layer issues of wide-band cognitive radio systems," in *2005 1st IEEE International Symposium on New Frontiers in Dynamic Spectrum Access Networks, DySPAN 2005*, pp. 151–159, usa, November 2005.

[13] W. A. Gardner, "Exploitation of spectral redundancy in cyclostationary signals," *IEEE Signal Processing Magazine*, vol. 8, no. 2, pp. 14–36, 1991.

[14] J. Lundén, V. Koivunen, A. Huttunen, and H. V. Poor, "Spectrum sensing in cognitive radios based on multiple cyclic frequencies," in *Proceedings of the 2nd International Conference on Cognitive Radio Oriented Wireless Networks and Communications (CrownCom '07)*, pp. 37–43, Orlando, Fla, USA, August 2007.

[15] Z. Khalaf, A. Nafkha, J. Palicot, and M. Ghozzi, "Hybrid spectrum sensing architecture for cognitive radio equipment," in *Proceedings of the 6th Advanced International Conference on Telecommunications (AICT '10)*, pp. 46–51, May 2010.

[16] L. S. Cardoso, M. Debbah, P. Bianchi, and J. Najim, "Cooperative spectrum sensing using random matrix theory," in *Proceedings of the 3rd International Symposium on Wireless Pervasive Computing (ISWPC '08)*, pp. 334–338, Santorini, Greece, May 2008.

[17] Y. Zeng and Y.-C. Liang, "Eigenvalue-based spectrum sensing algorithms for cognitive radio," *IEEE Transactions on Communications*, vol. 57, no. 6, pp. 1784–1793, 2009.

[18] F. Penna and R. Garello, "Theoretical performance analysis of eigenvalue-based detection," http://arxiv.org/abs/0907.1523.

[19] F. Liu, S. Guo, and Y. Sun, "Primary user signal detection based on virtual multiple antennas for cognitive radio networks," *Progress in Electromagnetics Research C*, vol. 42, pp. 213–227, 2013.

[20] V. Savaux, Y. Louët, M. Djoko-Kouam, and A. Skrzypczak, "Application of a joint and iterative MMSE-based estimation of SNR and frequency selective channel for OFDM systems," *EURASIP Journal on Advances in Signal Processing*, vol. 2013, article 128, 2013.

[21] P. Bello, "Characterization of randomly time-variant linear channels," *IEEE Transactions on Communications Systems*, vol. 11, no. 4, pp. 360–393, 1963.

[22] O. Edfors, M. Sandell, J.-J. D. van de Beek, S. K. Wilson, and P. O. Börjesson, "OFDM channel estimation by singular value decomposition," *IEEE Transactions on Communications*, vol. 46, no. 7, pp. 931–939, 1998.

[23] M. Biguesh and A. B. Gershman, "Downlink channel estimation in cellular systems with antenna arrays at base stations using channel probing with feedback," *Eurasip Journal on Applied Signal Processing*, vol. 2004, no. 9, pp. 1330–1339, 2004.

[24] S. Kay, *Fundamentals of Statistical Signal Processing: Estimation Theory*, Prentice-Hall, 2003.

[25] F. Iutzler and P. Ciblat, "Fully distributed signal detection: application to cognitive radio," in *Proceedings of the European Signal Processing Conference (EUSIPCO '13)*, 2013.

[26] S. M. Kay, *Fundamentals of Statistical Signal Processing: Detection Theory*, vol. 2, Prentice Hall, 1998.

[27] M. Abramowitz and I. Stegun, *Handbook of Mathematical Functions with Formulas, Graphs, and Mathematical Tables*, Dover, New York, NY, USA, 1970.

[28] V. I. Kostylev, "Energy detection of a signal with random amplitude," in *Proceedings of the International Conference on Communications (ICC '02)*, vol. 3, pp. 1606–1610, May 2002.

[29] F. F. Digham, M.-S. Alouini, and M. K. Simon, "On the energy detection of unknown signals over fading channels," *IEEE Transactions on Communications*, vol. 55, no. 1, pp. 21–24, 2007.

[30] ETSI, "Digital Radio Mondiale (DRM), system specification," Tech. Rep. ES 201 980 V 3.1.1, ETSI, 2009.

[31] Y. Zeng and Y.-C. Liang, "Spectrum-sensing algorithms for cognitive radio based on statistical covariances," *IEEE Transactions on Vehicular Technology*, vol. 58, no. 4, pp. 1804–1815, 2009.